# Precise Positioning for Automotive with Mass Market GNSS Chipsets

Lance de Groot, Eduardo Infante, Altti Jokinen, Brett Kruger, Laura Norman
*Hexagon Positioning Intelligence, Calgary, AB, Canada*

## BIOGRAPHIES

Lance de Groot holds a B.Sc. and M.Sc. in Geomatics Engineering from the University of Calgary. He joined Hexagon Positioning Intelligence (PI) in 2008 and has worked on ground reference receivers for SBAS networks, high precision positioning and relative alignment algorithms for commercial applications, and safety critical software for autonomous applications. He is currently a member of PI's Safety Critical Systems group.

Eduardo Infante is a Geomatics Engineer within PI's Safety Critical Systems group. He holds a B.Sc. in Geomatics Engineering from the University of Calgary and a M.Sc. in Geodesy and Geomatics Engineering from the University of New Brunswick. His research in his MSc. studies consisted in developing a loosely coupled INS solution using low grade GNSS and INS sensors found in smartphones.

Altti Jokinen is Senior Geomatics Designer in PI's algorithms group. He has over 11 years of experience on GNSS and its applications. He received his PhD degree from Imperial College London in 2015. His PhD studies focused to Precise Point Positioning (PPP) and his main research aims were reducing PPP solution convergence time, improving accuracy and integrity.

Brett Kruger is a Software engineer working within PI's Safety Critical Systems group. With his background in INS, he leads the development of ASIL rated inertial software targeting autonomous driving applications. Brett graduated with a MASc in Electrical engineering from the University of Toronto in 2012.

Laura Norman obtained her B.Sc and M.Sc. in Geomatics Engineering from the University of Calgary. Her research focused on investigating the performance of low-cost consumer grade GNSS receivers for position and trajectory length estimation. Since 2017 she has been a Geomatics Engineer in PI's Safety Critical Systems Group.

## ABSTRACT

GNSS chipsets currently in use in automotive applications are typically single frequency receivers offering a code phase solution which does not provide the accuracy required by emerging Advanced Driver Assistance Systems (ADAS), Autonomous Driving (AD), and Vehicle-to-Everything (V2X) applications. Several mass market GNSS receiver manufacturers have recently announced dual frequency chipsets using new civil signals. This paper presents results from using measurements from mass market dual frequency GNSS chipsets in NovAtel's (a part of Hexagon Positioning Intelligence) Precise Point Positioning (PPP) algorithms to improve the positioning accuracy and integrity to levels suitable for ADAS/AD applications.

Data was collected using mass market chipsets from three manufacturers in both static and kinematic scenarios. A zero-baseline static test was performed to characterize the measurement noise of each chipset, with results ranging from 15 to 57 cm for code noise, and 0.7 to 5.3 mm for phase noise, both up to 15x greater than a survey grade receiver. The increased code noise results in increased PPP convergence time. In kinematic testing, under open sky conditions, the horizontal position accuracy ranged from 28 cm to 36 cm at 95%. The use of these measurements in PPP represents an improvement over the code phase position provided by the chipset of 60-90%.

Convergence time is a known limitation of PPP algorithms, and is more pronounced with mass market chipsets due to high code measurement noise. Ionospheric corrections from a Regional Ionosphere Model (RIM) are supplied to reduce convergence time. For single frequency mass market chipsets, convergence to 1 metre at 95% is not achieved within 20 minutes without ionospheric corrections. With RIM corrections convergence to 1 metre (95%) can be achieved in less than

30 seconds. For a dual frequency chipset the time to converge to 1 metre (95%) is reduced from 9 minutes to less than 30 seconds. The antenna can also have a significant impact on performance. The convergence performance is compared between a geodetic grade antenna and a representative automotive grade antenna in static moderate multipath environments.

In summary, this paper illustrates that measurements from mass market GNSS chipsets may be used with NovAtel's PPP algorithm and TerraStar-X corrections to achieve the performance demanded by ADAS/AD and V2X applications, and that corrections from a RIM permit convergence times of less than one minute for both single and dual frequency chipsets, a necessary feature for automotive applications.

## INTRODUCTION

The majority of GNSS chipsets used in production automotive applications today are single frequency, offering a code phase only position with an accuracy on the order of five to ten metres. The primary application of these chipsets is for infotainment and route navigation applications. However, emerging automotive applications are imposing requirements for higher accuracy. The proposed requirements for horizontal position accuracy in Vehicle-to-Vehicle (V2V) communications are 1.5 m in latitude and longitude at 68% [1]. Requirements for position accuracy in Advanced Driver Assistance Systems (ADAS) and Autonomous Driving (AD) are likely to be even higher, requiring positions accurate enough for navigation within a lane, understood to be less than one metre.

At the same time, the launch of modernized GPS and new constellations have made possible dual frequency receivers using only civil signals. Previously, dual frequency receivers had been the domain of specialized manufacturers with access to semi-codeless tracking technology. Several mass market GNSS receiver manufacturers have recently announced dual (or triple) frequency chipsets. The advent of dual frequency mass-market chipsets raises the possibility of attaining higher accuracies in automotive and other mass market applications.

Even with additional frequencies, a code phase solution alone will not be sufficient to achieve the sub-metre accuracy demanded by AD/ADAS applications. Carrier phase positioning will be required to achieve these accuracies. In this work we combine measurements from single and dual frequency mass market GNSS chipsets with NovAtel's (a part of Hexagon Positioning Intelligence) PPP algorithm [2], [3] and TerraStar-X corrections to assess the feasibility of carrier phase positioning with these chipsets. We also make an initial examination of the impact of using and automotive grade antenna, as compared to a survey grade antenna.

In addition to the GNSS receiver, mass-market inertial measurement units (IMU) are also becoming more widely available and are achieving improved performance. We anticipate that new mass market IMUs will be combined with mass-market GNSS chipsets in emerging applications. A discussion of IMU performance is beyond the scope of this work, but is examined in related research [4].

## CHIPSETS UNDER EVALUATION

This study uses four mass market chipsets from three manufacturers. As some of these chipsets have not yet been released and the performance shown here may not represent final performance, none are specifically identified. The authors present the performance attained across the set of chipsets as an indication of the potential performance with NovAtel's PPP algorithms and mass market chipsets in general, rather than focusing on any specific receiver.

The chipsets are:

- Chipset A: an L1 only chipset
- Chipset B: a L1/L2 chipset from the same manufacturer as chipset A
- Chipset C: an L1 only chipset from a different manufacturer
- Chipset D: an L1/L5 chipset from a third manufacturer

The software used for chipsets A and C supported GPS L1 C/A and GLONASS L1, and for chipsets B and D all available civil signals in the listed bands from GPS, GLONASS, and Galileo. Chipsets A, C, and D were housed in manufacturer supplied evaluation kits. Chipset B was placed on a manufacturer supplied RF board and mounted on a communications carrier board designed at NovAtel.

## MEASUREMENT NOISE

A static zero-baseline double difference was conducted with all four chipsets to characterize their measurement noise. Measurements were collected for 30 minutes from each receiver pair using a NovAtel prototype dual-frequency automotive grade antenna. Measurement noise is summarised in Table 1. Statistics are shown only for GPS and GLONASS L1 signals, as these are the only signals supported by all chipsets, to enable direct comparison. Performance for other signals is anticipated to be consistent, considering differences due to signal structure. A NovAtel OEM729 is included for reference.

Table 1: Measurement Noise Summary

| | Code Phase Standard Deviation (cm) | | Carrier Phase Standard Deviation (mm) | |
|---|---|---|---|---|
| | GPS L1 C/A | GLS L1 CA | GPS L1 C/A | GLS L1 |
| Chipset A | 15 | 29 | 1.7 | 2.0 |
| Chipset B | 26 | 52 | 1.8 | 2.3 |
| Chipset C | 16 | 33 | 0.7 | 2.2 |
| Chipset D | 49 | 57 | 3.3 | 4.7 |
| OEM729 | 5 | 4 | 0.5 | 0.6 |

Code phase standard deviation ranges from 15 cm to 57 cm across the set of chips, or 3 to 14 times greater than the NovAtel survey grade reference receiver. This increase in code noise is expected due to the need for less expensive analog filtering resulting in a narrower front-end bandwidth, which imposes wider correlator spacings [5]. This is expected to result in slower convergence in PPP processing because the code must be averaged in the filter in order to estimate the carrier phase ambiguity. The use of a wider correlator spacing also indicates that the mass market chipsets will be more susceptible to code multipath error [5].

Phase noise ranges from 0.7 mm to 5.3 mm, or 1.5 to 15 times the NovAtel reference. Front-end bandwidth and correlator spacing do not have the same effect on phase noise and the closer performance to the reference is also expected. The phase noise increase is only at the mm level, which will not be dominant in a PPP solution having an accuracy of several cm, and thus is not expected to have a significant impact on converged performance.

## CONVERGENCE PERFORMANCE

A comparatively long convergence time is a known limitation of PPP algorithms, as compared to code phase positioning, or Real Time Kinematic (RTK) techniques using observation space corrections. A significant reason for the convergence time is the need to average the code phase measurements to estimate the carrier phase ambiguity. We find that this is more pronounced with mass market chipsets due to higher code measurement noise and multipath as compared with the survey grade receivers typically used in PPP applications.

Convergence times of many minutes are not acceptable for automotive applications, where there is an expectation that the vehicle must be operable very shortly after being started. The TerraStar-X service can be used to overcome this problem. TerraStar-X provides ionosphere corrections from a regional ionospheric model (RIM) and significantly improves convergence time even with survey grade receivers [6]. As the TerraStar-X service is still in a trial phase it does not currently include corrections for L5 signals. As such, results presented here and in the next section for chipset D are L1 only, despite chipset D being L1/L5 capable.

Multiple days of data were collected for each chipset in a low multipath environment on the rooftop of NovAtel's headquarters. Results for chipsets A, B, and C, and the OEM7 reference were collected using a NovAtel prototype L1/L2 automotive grade antenna. For receiver D data was collected using a NovAtel 704 wideband survey grade antenna in order to include the L5 band. In the low multipath environment of these tests the difference in antenna is not expected to be significant because the differences in axial ratio and low elevation gain primarily affect the amount of multipath received (refer to Antenna Impact section below).

The data were processed offline through NovAtel's PPP algorithm with simulated filter resets every 20 minutes to observe the convergence behaviour over many samples. Figure 1 shows the 95% confidence horizontal convergence performance for all chipsets without regional ionospheric corrections; i.e. with only clocks, orbits, and biases. For the single frequency chipsets A and C and the single frequency solution from chipset D, the solution does not reliably converge to a 1 metre level within 20 minutes. This is a result of the lack of any ionospheric information. Even for the dual frequency chipset B where the ionospheric delay can be estimated from the dual frequency measurements, convergence time to 1 metre is nearly 9 minutes. In comparison, the NovAtel OEM7 (also using L1/L2) converges within 40s. This demonstrates the impact of the increased code-phase noise of the mass-market chipset vs. the survey grade reference.

Figure 2 shows the 95% confidence horizontal convergence performance for all chipsets with regional ionospheric corrections from the TerraStar-X service. Figure 3 provides a closer look at the initial convergence period for the same data. Table 2 summarises the performance and improvement afforded by the RIM corrections for all receivers. The addition of regional ionospheric corrections greatly improves the convergence performance of all receivers, including the OEM7 reference. For all but one of the mass-market chipsets it is now possible to achieve a 1m error at 95% confidence in less than 30s, making the solution feasible for automotive applications.

It is of interest to note that the dual frequency chipset B now has comparable performance to chipset C. This is a consequence of the accuracy of the ionosphere corrections, and the lower code-phase noise of chipset C. When the ionosphere corrections are very accurate the additional information provided by the second frequency is not as significant, and the contribution of lower code-phase noise to improved convergence is more so. We anticipate that the benefits of a dual frequency chipset will be more pronounced in more ionospherically active regions, as the solar cycle returns to a maximum, when estimating and correcting the ionospheric delay will be more difficult.

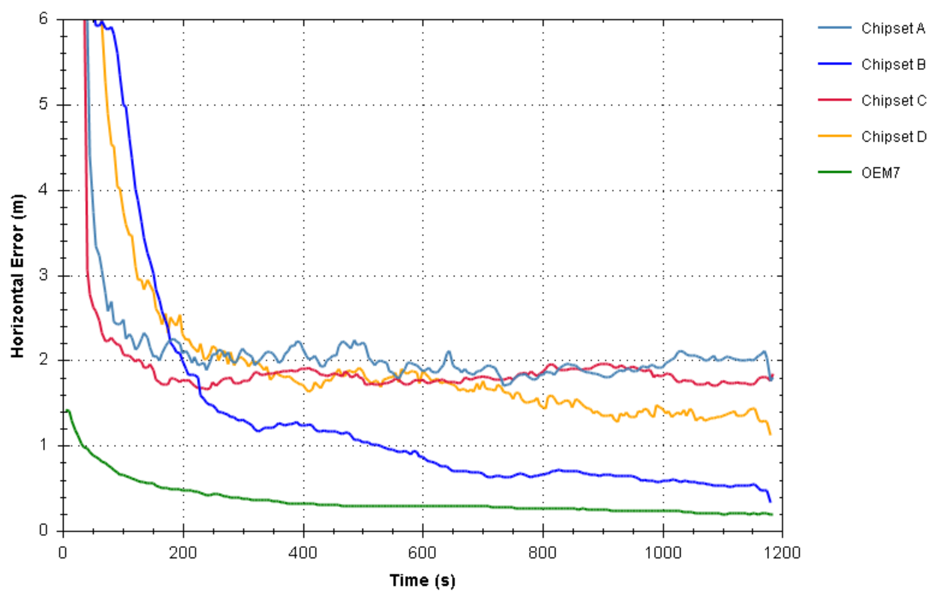


Figure 1: 95% Horizontal Convergence Performance without Ionosphere Corrections

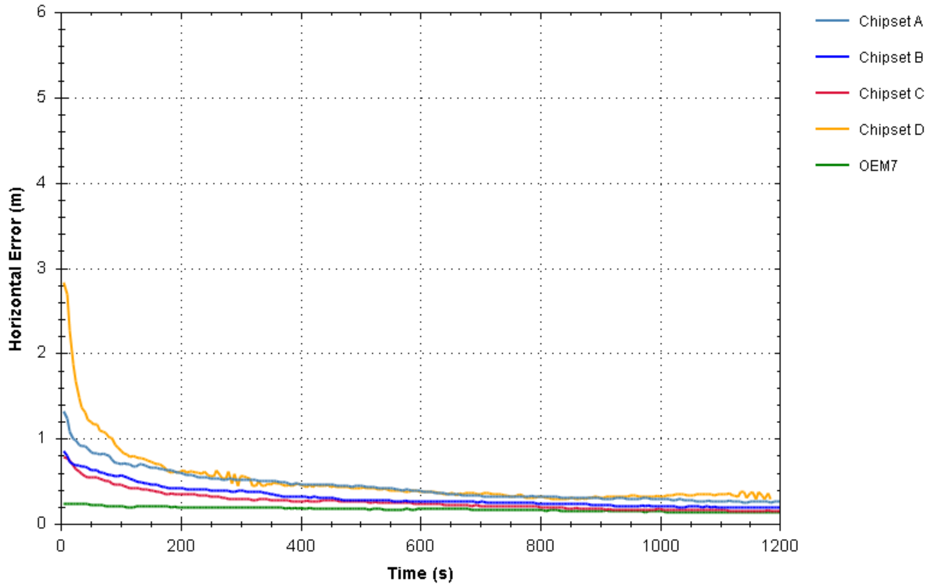


Figure 2: 95% Horizontal Convergence Performance with Ionosphere Corrections

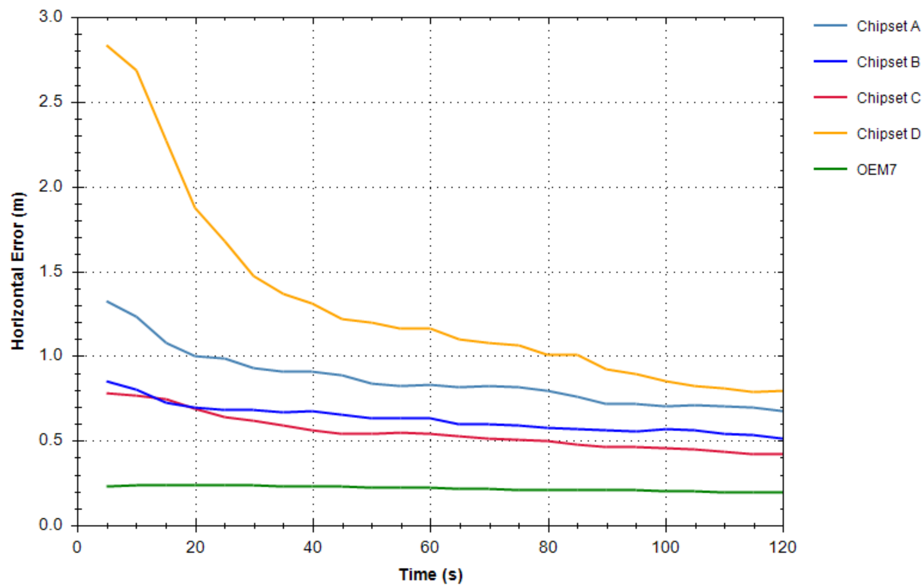


Figure 3: 95% Horizontal Convergence Performance with Ionosphere Corrections, Detail

Table 2: 95% Horizontal Convergence Summary

| | 95% horizontal error after 60 s (m) | | Improvement |
|---|---|---|---|
| | Without RIM | With RIM | |
| Chipset A | 3.2 | 0.8 | 75% |
| Chipset B | 5.9 | 0.6 | 90% |
| Chipset C | 2.5 | 0.5 | 80% |
| Chipset D | 6.3 | 1.16 | 82% |
| OEM7 | 0.8 | 0.2 | 75% |

## POSITIONING PERFORMANCE

Kinematic testing was conducted in a variety of environments to assess the positioning performance that can be achieved with mass-market chipsets and PPP techniques. A test setup suitable for kinematic testing with chipset D was not available, and so results are presented only for the first three chipsets.

Kinematic testing was conducted with a NovAtel test van, with roof mount points for antennas. A 6-way antenna splitter was used to feed the signals from a NovAtel prototype dual frequency automotive grade antenna to the chipsets under test. The truth system consisted of a NovAtel OEM729, a Litef uIMU motion sensor, and a survey grade GPS-702-GGL antenna mounted roughly one metre apart from the automotive grade antenna. The raw GNSS and IMU data from the truth system were post-processed in Waypoint Inertial Explorer and offset to the location of the automotive grade antenna to produce a reference trajectory against which the results from the chipsets under test were compared.

Raw measurements were collected from each chipset and were processed together with ephemeris and TerraStar-X corrections with an offline version of NovAtel's real time algorithms.

### Open Sky Environment

An open sky kinematic test was performed in an industrial district north of the Calgary airport. The route is a mix of single storey warehouses and a short section of controlled access freeway excluding any underpasses. The test trajectory is shown in Figure 4. Epochs outside the open sky trajectory shown are filtered from these results, to assess the performance only under the open sky condition.

Figure 4: Open sky test trajectory [7]

A time series of horizontal position error for the three chipsets is shown in Figure 5. A CDF is shown in Figure 6. Table 3 summarizes the performance.

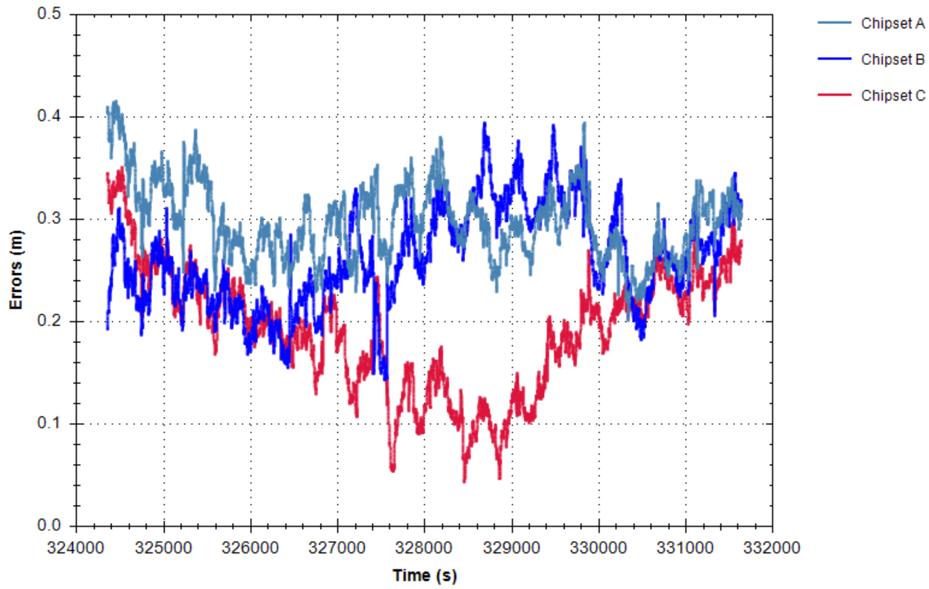


Figure 5: Horizontal Position Error – Open Sky Trajectory

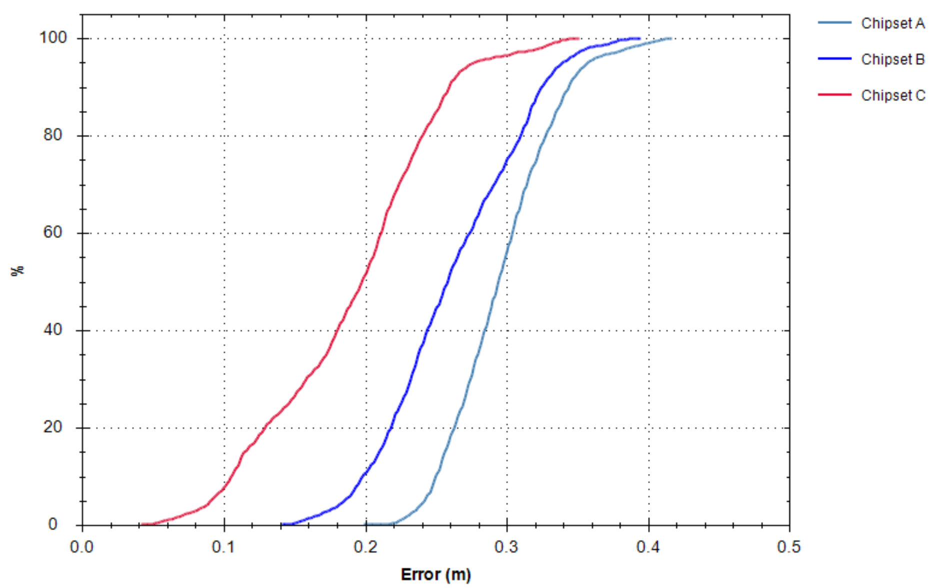


Figure 6: Horizontal Error CDF – Open Sky Trajectory

PPP processing with all three chipsets yields horizontal error less than 40 cm. The divergence between chipset C and the other chipsets beginning at time 327000 is caused by differences in tracking behaviour between the chipsets when passing under a pair of overhead signs around this time. Minor differences in behaviour between the chipsets are typical, but overall performance is similar when aggregated across a variety of tests, as is seen in the subsequent sections.

Figure 7 shows a comparison of the horizontal error for the chipset's on-board SBAS-corrected solution and the NovAtel PPP solution with the same measurements, demonstrating the potential for performance improvement when applying PPP techniques with these chipsets. Chipset B is shown here as an example, results for the other chipsets are similar and are summarised in the subsequent tables. This figure shows the potential to achieve the requirements of emerging automotive applications using mass-market receiver hardware by combining it with Hexagon's positioning algorithms and correction services.

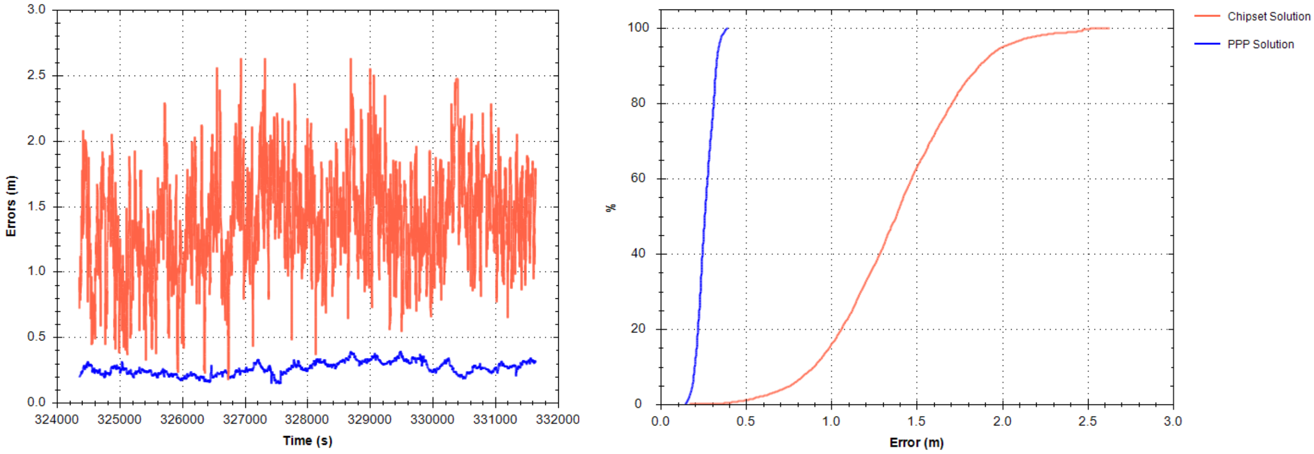


(a) (b)

Figure 7: Time Series (a) and CDF (b) Comparison between Chipset B On-board Solution and NovAtel PPP Solution

Table 3: Horizontal Error Summary – Open Sky Trajectory

| | PPP Horizontal Error | | Chipset Solution Horizontal 95% Error | Improvement with NovAtel PPP algorithm |
|---|---|---|---|---|
| | 68% (m) | 95% (m) | | |
| Chipset A | 0.31 | 0.36 | 4.99 | 93% |
| Chipset B | 0.29 | 0.34 | 2.01 | 83% |
| Chipset C | 0.22 | 0.28 | 0.77 | 64% |

**Highway Environment**

A highway kinematic dataset was collected along Deerfoot Trail (Hwy 2) and Stoney Trail, two of the main freeways within the city of Calgary. This route, shown in Figure 8, consists of generally open sky punctuated by frequent total GNSS outages from passing under overpasses.

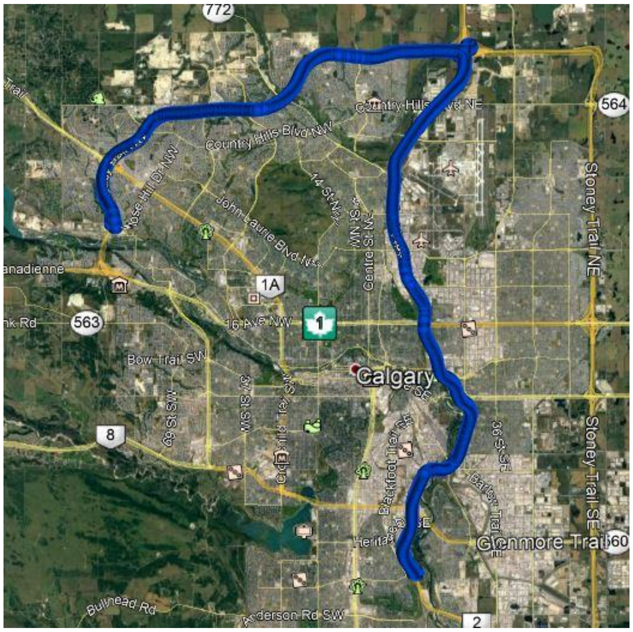


Figure 8: Highway Test Trajectory with Frequent Overpasses [8]

A time series of horizontal position error for the three chipsets is shown in Figure 9. A CDF is shown in Figure 10. Table 4 summarizes the performance.

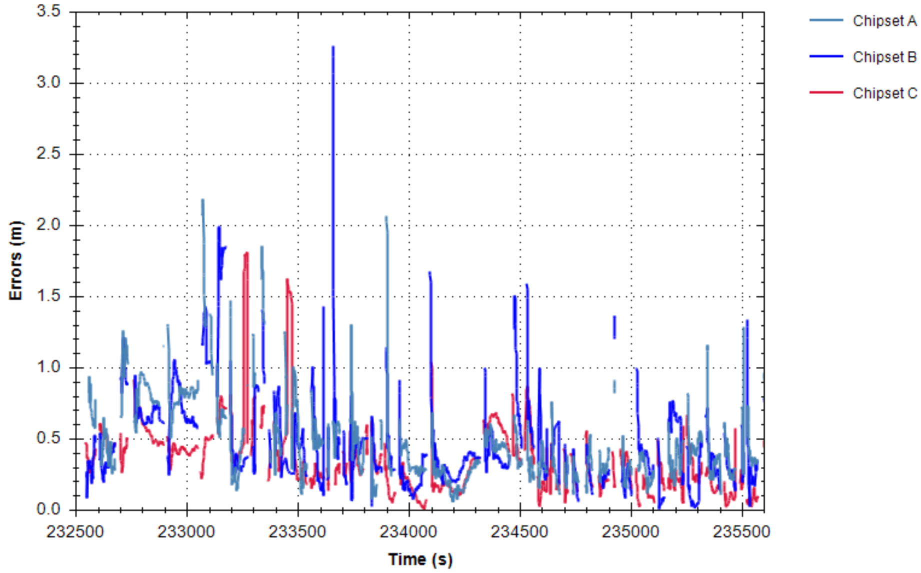


Figure 9: Horizontal Position Error – Highway Trajectory with Frequent Overpasses

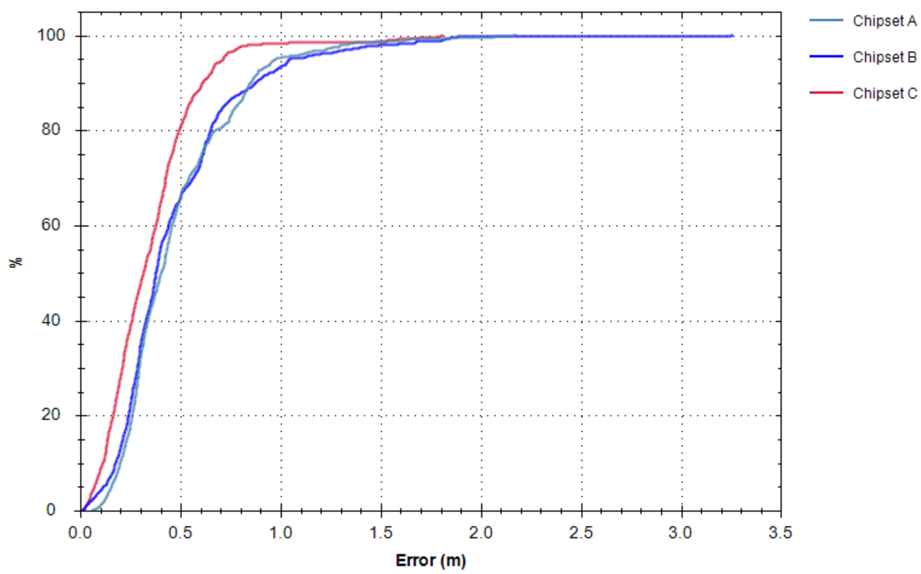


Figure 10: Horizontal Error CDF – Highway Trajectory with Frequent Overpasses

Horizontal PPP error for all chipsets in highway environments is around 1.0 m at 95%. As expected this value is larger than that seen in the open sky environment due to the multiple reconvergence periods that occur after a loss of lock caused by each overpass. This highlights the impact of the increased code noise of mass-market chipsets on the attainable performance. The higher code noise results in a longer reconvergence time after each outage, and a lower aggregate performance than could be obtained with a mass market chipset. Regardless, the performance for all chipsets is still less than 1 m, which shows promise for AD/ADAS applications, especially if combined with an IMU or other relative positioning technology to bridge GNSS outages.

Table 4: Horizontal Error Summary – Highway Trajectory

| | PPP Horizontal Error | | Chipset Solution Horizontal 95% Error | Improvement with NovAtel PPP algorithm |
|---|---|---|---|---|
| | 68% (m) | 95% (m) | | |
| Chipset A | 0.52 | 0.98 | 1.12 | 12% |
| Chipset B | 0.53 | 1.05 | 1.65 | 36% |
| Chipset C | 0.42 | 0.71 | 1.22 | 42% |

**Suburban Environment**

Suburban data was collected in the residential neighborhoods of north-central Calgary. The route taken is displayed in Figure 11. This route has fewer complete GNSS outages than the highway trajectory but has more partial outages and partial tree cover throughout the test route.

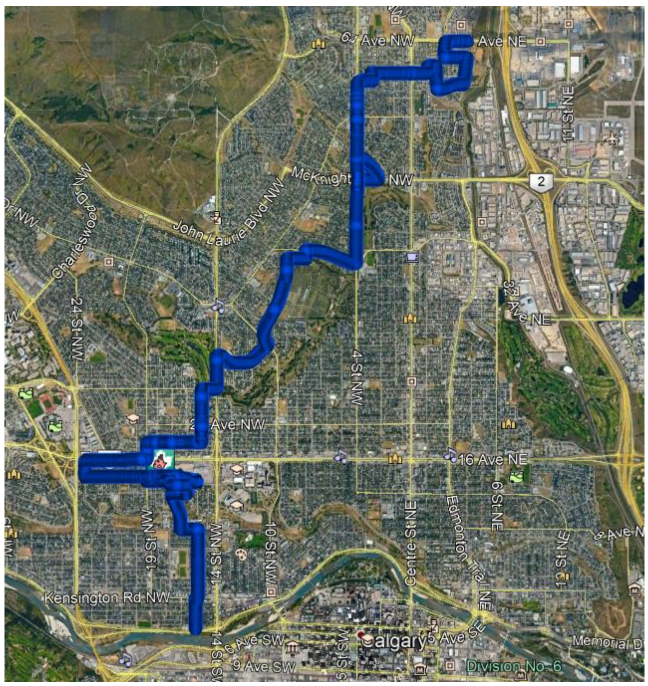


Figure 11: Suburban test trajectory [9]

A time series of horizontal position error for the three chipsets is shown in Figure 12. A CDF is shown in Figure 13. Table 5 summarizes the performance.

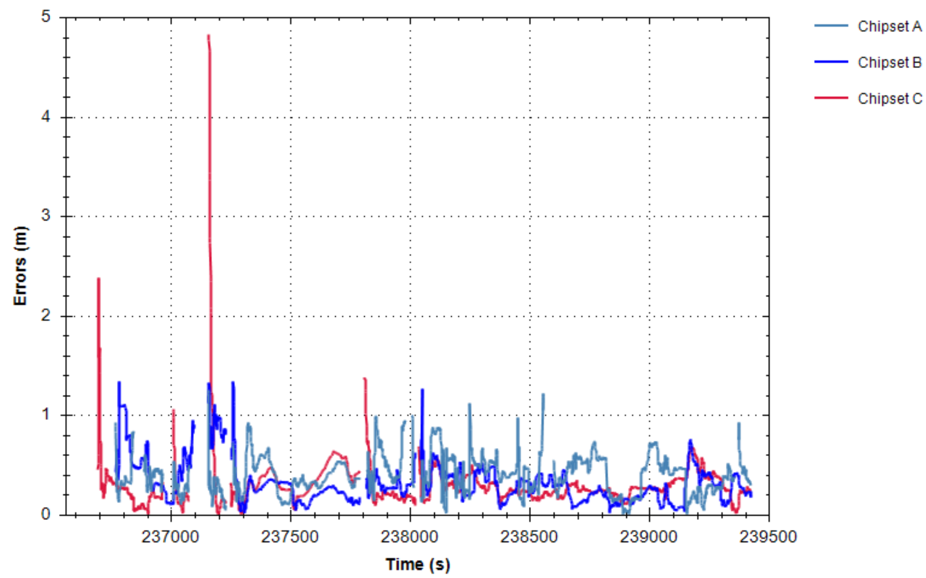

Figure 12: Horizontal Position Error – Suburban Trajectory

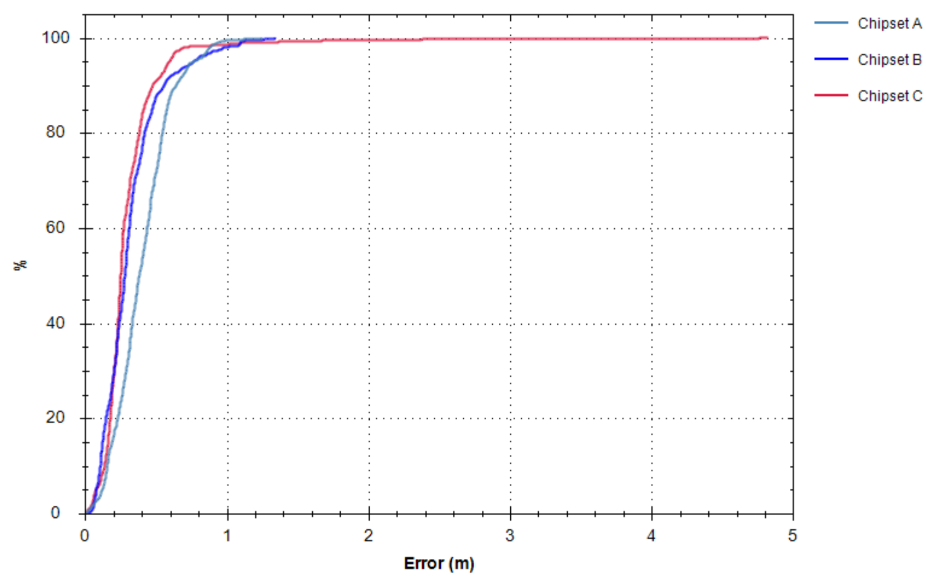

Figure 13: Horizontal Error CDF – Suburban Trajectory

As with the highway section the PPP solution had a 95% error less than 1.0 m for all chipsets. In this environment however the error is driven by a generally higher level of error from foliage and multipath, rather than by frequent reconvergence. Some reconvergence still occurs, for example at time 237180, noted by the spike in the error series for chipset C, which is typical of the start of a convergence period, and is accompanied by a higher estimated standard deviation from the filter. Overall the results obtained were comparable between all three units being tested.

Table 5: Horizontal Error Summary – Suburban Trajectory

| | PPP Horizontal Error | | Chipset Solution Horizontal 95% Error | Improvement with NovAtel PPP algorithm |
|---|---|---|---|---|
| | 68% (m) | 95% (m) | | |
| Chipset A | 0.48 | 0.77 | 1.83 | 58% |
| Chipset B | 0.34 | 0.77 | 1.27 | 39% |
| Chipset C | 0.31 | 0.60 | 2.53 | 76% |

**ANTENNA IMPACT**

The introduction of mass market dual frequency chipsets will create a need for mass market dual frequency antennas as well. While the use of a mass-market GNSS chipset rather than a survey grade receiver has obvious implications on positioning performance, the performance of the antenna in use will also have a significant impact. Antennas used in production automotive applications today are almost exclusively small, single frequency, passive patches. We anticipate that even as multi frequency GNSS is adopted by the automotive sector the antennas will continue to be passive patches with as small a footprint as possible. These antennas can be expected to have less stable phase centres, slower low-elevation roll-off, and a lower axial ratio than antennas used in surveying and other current high precision applications. In this work we focus on the effect of multipath, but other impacts from the antenna may also be applicable.

To observe the effect of the antenna, we conducted static tests in two moderate multipath environments with two different antennas: a survey grade NovAtel GPS-702-GGL pinwheel antenna [10], and a NovAtel prototype dual frequency automotive grade antenna. The automotive grade antenna is an L1/L2 passive patch antenna element designed to be capable of manufacture at mass-market volumes and with automotive grade components. Each antenna was split to two receivers. As the intent of this test is to observe the impact of the antenna, only the NovAtel OEM729 reference receiver and chipset B were used in this test; we anticipate that the results would be similar for other mass-market chipsets.

The L1 frequency gain patterns of the two antennas are shown in Figure 14. The automotive grade antenna (b) has a more gradual roll-off below 0° elevation than the GPS-702-GGL (a); an important factor to mitigate the effect of ground reflected multipath. As well, the axial ratio of the automotive grade antenna is lower than the GPS-702-GGL, resulting in higher gain of reflected signals at all elevations. From both these factors we can anticipate that the impact of multipath will be greater with the automotive grade antenna. The L2 gain patterns are not shown but have similar trends.

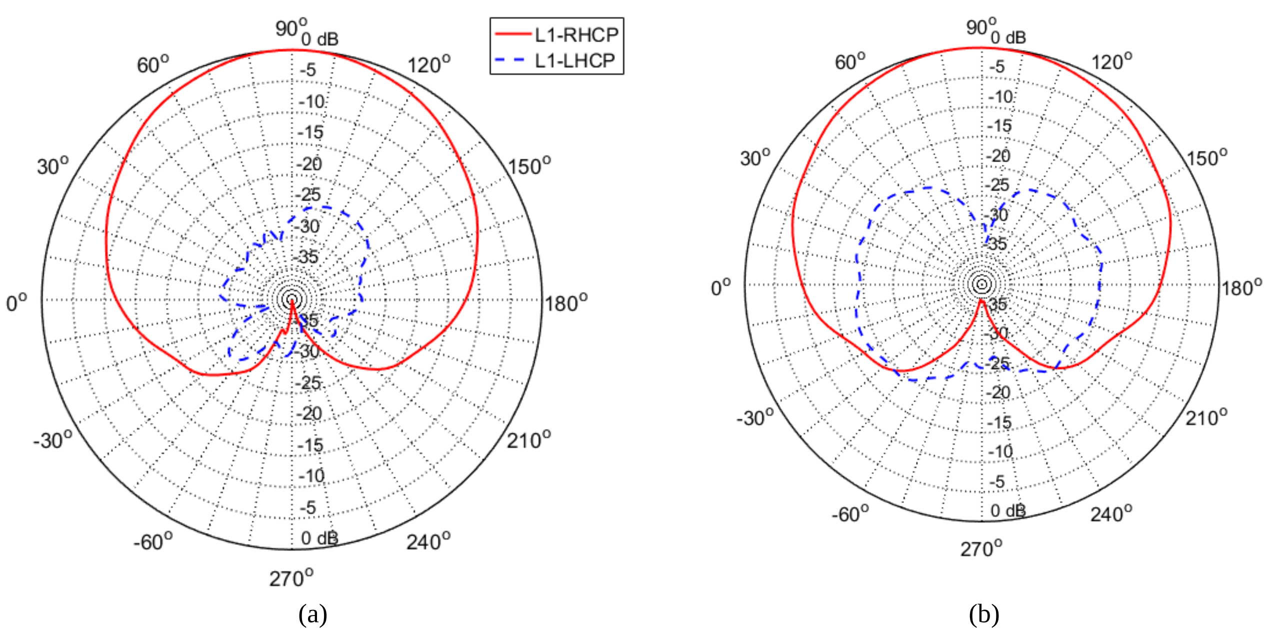


Figure 14: L1 Gain Pattern of GPS-702-GG (a) and Prototype Automotive Grade Antenna (b)

The first test was conducted in an open parking lot between a 3 storey and two storey building, approximately 100 metres from the former and 35 metres from the latter. The second test was conducted in the parking lot of NovAtel's two storey headquarters, approximately 20 metres from the nearest face of the building, and 60 metres from an adjoining face. Figure 15 shows the test locations.


(a)

(b)

Figure 15: Moderate Multipath Test Environments for Antenna Tests 1 (a) and 2 (b)

As the impact of multipath is greatest on the code-phase, which is most significant during convergence, data were processed offline with simulated PPP filter resets every 5 minutes to observe the impact of the antenna on convergence time. Figure 16 and Figure 17 show the 68% horizontal convergence performance for the two tests.

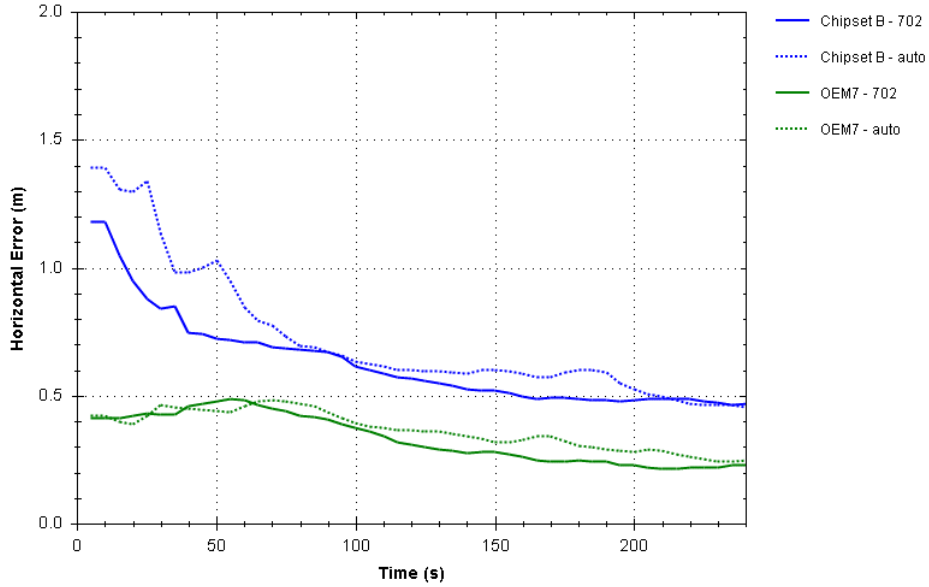


Figure 16: 68% Horizontal Convergence Performance under Moderate Multipath – Test 1

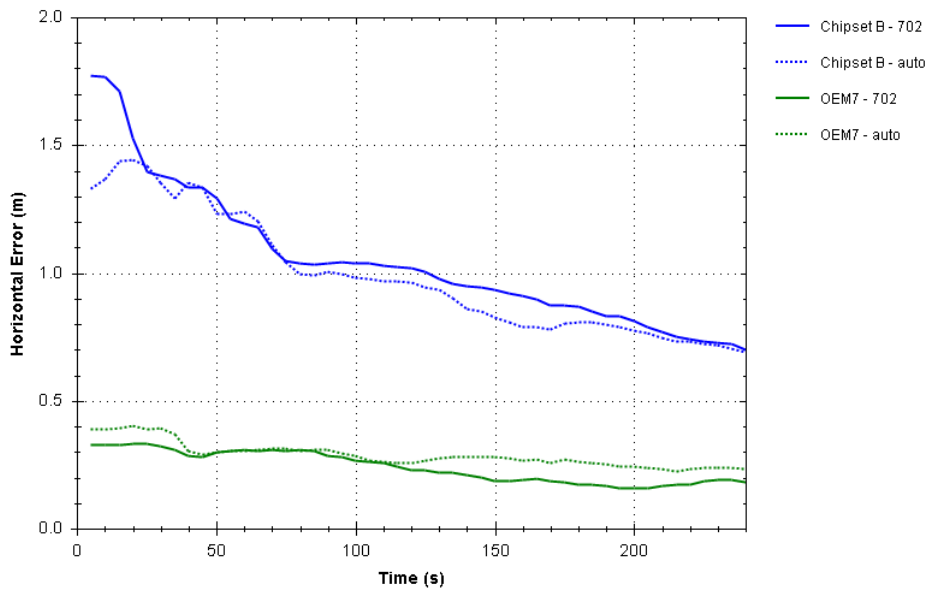


Figure 17: 68% Horizontal Convergence Performance under Moderate Multipath – Test 2

The behaviour is inconsistent between the tests, likely due to the difference in the geometry and reflecting environment between the two tests. The most significant impact occurs in the first 100 s of convergence on chipset B in the first test, where the performance with the automotive grade antenna is 20% worse after 60s than with the GPS-702-GGL. The OEM7 also shows slightly worse performance with the automotive grade antenna, but not as significantly as chipset B. This is to be expected if the impact of the antenna is primarily in multipath rejection; the front-end differences between the receivers that lead to higher code noise in the mass-market receivers also limit their ability to mitigate multipath as compared to a survey grade receiver. In general, these results indicate that antenna selection will have an impact on automotive applications with mass-market chipsets, but further analysis under more controlled multipath conditions is required to attain conclusive results.

## CONCLUSIONS

In summary, we show that while measurements from mass-market GNSS chipsets have higher noise than the survey grade receivers currently used in most PPP applications, when combined with NovAtel's PPP algorithm the mass-market chips can achieve the positioning performance demanded by ADAS/AD and V2X applications. Ionospheric corrections, e.g. from the TerraStar-X service, are necessary to achieve convergence times of less than one minute for both single and dual frequency chipsets, a necessary feature for automotive applications. Lastly, we present some evidence to confirm the expectation that the wider correlator correlator spacing of the mass-market chips causes them to be more affected by the reduced multipath mitigation afforded by automotive grade antennas. This suggests that antenna selection is an important consideration in applications with mass-market chipsets, but further investigation is required.

## ACKNOWLEDGMENTS

The authors wish to thank the manufacturers of the mass market chipsets used in this work for providing early access to newly developed dual frequency receivers, and for their support in working with these receivers.

## REFERENCES

1. National Highway Traffic Safety Administration, Department of Transportation (DOT), "Federal Motor Vehicle Safety Standards; V2V Communications," Notice of Proposed Rulemaking (NPRM). NHTSA-2016-0126, RIN 2127-AL55, 2016.
2. Jokinen, A., Ellum, C., Neumann, J., Chan, D., Webster, I., Masterson, S. and Morley, T., "Kinematic performance of NovAtel CORRECT with terrastar-D Precise Point Positioning (PPP) service," *Proceedings of the 27th International Technical Meeting of the Satellite Division of the Institute of Navigation (ION GNSS+ 2014) Tampa, FL, September 2014*, pp. 1020-1034.
3. Jokinen, A., Ellum, C., Webster, I., Masterson, S. and Morley, T., "NovAtel CORRECT with Precise Point Positioning (PPP) for High Accuracy Kinematic Applications," *Proceedings of the 28th International Technical Meeting of the Satellite Division of the Institute of Navigation (ION GNSS+ 2015) Tampa, FL, September 2015*, pp. 1123-1152.
4. Dixon, R., Bobye, M., Kruger, B., and Sinha, S., "GNSS/INS Fusion for Automotive with Mass Market Sensors," *Proceedings of the International Meeting of the Satellite Division of The Institute of Navigation (ION GNSS+ 2018), Miami, FL, September 2018, pp. TBD.*
5. Van Dierendonck, A. J., Fenton, P. and Ford, T., "Theory and Performance of Narrow Correlator Spacing in a GPS Receiver", *Navigation: Journal of the Institute of Navigation, Vol. 39, No. 3, Fall 1992.*
6. Jokinen, A., Ellum, C., Webster, I., Shanmugam S. and Sheridan, K., "NovAtel CORRECT with Precise Point Positioning (PPP): Recent Developments," *International Meeting of the Satellite Division of The Institute of Navigation (ION GNSS+ 2018), Miami, FL, September 2018.*
7. Source: "Figure 4: Open sky test trajectory," *Google Earth*, 31 August, 2017, accessed 12 September, 2017.
8. Source: "Figure 8: Highway test trajectory," *Google Earth*, 31 August, 2017, accessed 12 September, 2017.
9. Source: "Figure 11: Suburban test trajectory," *Google Earth*, 31 August, 2017, accessed 12 September, 2017.
10. NovAtel Inc, "GPS-701-GG & GPS-702-GG," [Data Sheet], available at https://www.novatel.com/assets/Documents/Papers/GPS701_702GG.pdf, accessed 12 September 2017.